Nonlinear Optical Properties of Water-Soluble Polymeric Dyes with Biological Applications

O. Varnavski,[†] **R. G. Ispasoiu,**[†] **M. Narewal,**[†] **J. Fugaro,**[‡] **Y. Jin,**[†] **H. Pass,**[‡] **and T. Goodson III***[,†]

Department of Chemistry, Wayne State University, Detroit, Michigan 48202, and Department of Surgery, Wayne State University School of Medicine, Detroit, Michigan 48202

Received November 4, 1999; Revised Manuscript Received March 20, 2000

ABSTRACT: The nonlinear optical properties of two water-soluble polymeric dyes, poly(R-478) (an anionic anthraquinone dye) and poly(S-119) (an anionic azo dye), are investigated utilizing nanosecond and femtosecond optical techniques such as *z*-scan, nonlinear transmission, and time-resolved luminescence. Poly(R-478) showed large nonlinear refraction when studied with femtosecond laser pulses at 800 nm, with a value for the intensity-dependent refractive index (n_I) of 1.26×10^{-4} cm^2/GW. The thin film result at 1064 nm indicated a large nonlinear absorption in both polymeric dyes. The origin of the large fast optical nonlinearities in the polymeric system S-119 was investigated by probing the different functional groups of the polymer. The chromophore group (Sunset Yellow) of the S-119 polymer showed a smaller nonlinear response when compared to the polymer result. Significant differences in the electronic dynamics between the parent poly(S-119) and the chromophore Sunset Yellow were observed by time-resolved luminescence spectroscopy. The applications of the NLO effects in these polymers are demonstrated for laser ablation of A549 lung carcinoma cells.

Introduction

Conjugated polymers are now important materials for potential applications in nonlinear optics (NLO), optical limiting, light emitting diodes, and photorefractive effects.[1−4] The advances in experimentation and conceptual understanding obtained from the vast research of NLO polymeric materials provide a strong basis for further investigations of new and useful macromolecular materials. Applications in self-assembled monolayers, NLO effects from surfaces, and the quantitative analytical characterization of materials and substances have already been demonstrated.[5−8] However, there have been no reports concerning the application of NLO effects in organic polymers to the characterization and ablation of biological materials.

There are several factors that may inhibit the use of organic NLO polymers in biological systems. There is a synthetic limitation due to the fact that most NLO organic polymers are not soluble in the aqueous phase. It is essential that organic polymers have suitable solubility with the biological system (in water) in order to probe real processes in the biological host. Another limiting factor is that many organic polymers possess structural characteristics that are toxic to the biological system used in the study. Indeed, it is important to analyze the biological material in its full and living condition without the difficult and confusing circumstance of cell death due to toxicity of the NLO polymer. The third major limitation of applying NLO effects to the characterization of biological systems is that the intensities necessary to detect large NLO effects in many materials are too large and potentially destructive to the biological host. It is crucial to find NLO polymers with very large nonlinear coefficients that require only small average powers (but perhaps larger peak intensities) to be used in order to detect appreciable NLO effects. All of these limitations should be overcome before significant advances in the application of organic polymeric NLO effects (and the understanding of the effects) to biological systems can be accomplished.

Recently, there have been advances toward the synthetic versatility of novel conjugate polymers with large NLO effects in the aqueous phase. Tripathy and coworkers[9] have reported large NLO effects with an epoxy-based polymer with NLO azo chromophores designed to contain anionic groups to induce water solubility and self-assembly. Using this polyanion with a polycation, multilayers were prepared on a glass substrate by alternating adsorption from dilute aqueous solutions. Heflin et al.[5] have utilized water-soluble NLO polymers for an ionically self-assembled monolayer (ISAM) technique for thin-film deposition. The second-harmonic intensity of the films exhibits the expected quadratic dependence on film thickness up to at least 100 bilayers, corresponding to a film thickness of 120 nm.[5] Tian et al.[10] have investigated the spectroscopic properties of a supramolecular system consisting of two oppositely charged porphyrin monomers, zinc tetrakis(4-sulfonoatophenyl)porphyrin and zinc tetrakis(*N*-methylpyridyl)porphyrin, by absorption and fluorescence spectroscopy. Photoinduced electron transfer and charge separation in the supramolecular system was studied by time-resolved degenerate four-wave mixing (DFWM), and the results indicated the formation of the charge-separated state within 30 ps and the recombination time is about 340 ps. There have been a number of other reports concerning the NLO effects of self-assembly systems based on water-soluble polymers such as the work by Fox et al.[11] in which molecules with cores of copper and nickel (octaazaphthalocyanines) are fused to four nonracemic helicenes.[11] The Langmuir−Blodgett films constructed from these systems give very large second-order NLO responses.[12] It is worth noting that

---

[†] Wayne State University.

[‡] Wayne State University School of Medicine.

* To whom all correspondence should be sent. E-mail: tgoodson@chem.wayne.edu.

10.1021/ma991868g CCC: $19.00

there have been no reports of organic NLO polymers exhibiting large effects in aqueous solution in the presence of biological systems.

A common source for dipolar macromolecular materials that are soluble in water and generally biologically inert and nontoxic is the use of food dyes. Two particular systems that have considerable promise are the polymeric dyes poly(S-119) and poly(R-478) (shown in Figure 1a,b).[13a,b]

As can be seen from the structures, these systems possess the necessary functionalities for large electronic NLO effects, due to their large degree of conjugation and the existence of dipolar groups on the side chains. Their suitable solubility (accomplished by the side groups with the $Na^+SO_3^-$ group) overcomes the first limitation as referred to above. Concerning their toxicity to cellular organisms it is interesting to note that these systems have already been used as markers (or tracers) in biological systems. Stahl et al.[14] have used the polymeric dye R-478 for studies in the developing small intestine. In this work the polymer was used as a marker in absorption studies in a food-free rat intestine. The results showed that polymer R-478 could provide a visible in vivo reference and can be easily recovered and accurately quantified over a wide range of concentrations. This suggested a relatively good nontoxic behavior of the polymeric dye in the biological system. Ball and Calton[15] have investigated the ability of a range of actinomycetes to decolorize the polymeric dye R-478. Three well-characterized ignocellulose-degrading actinomycetes were found to be the most efficient at decolorizing the polymer. Extracellular fractions taken from the actinomycete grown on a variety of lignocellulose-related substrates were also capable of decolorizing poly(R-478), indicating that dye decolorization was not merely due to biomass uptake.[15] It can be seen from these reports and others reported in the literature[16,17] (as well as our initial work on poly(R-478) with neoplastic tissues[18]) that the polymers R-478 and S-119 are not toxic at moderate concentrations and are strongly associated into the cell structure of the biological sample. However, there have been no reports of the ultrafast (femtosecond) NLO of these polymeric dyes that hold promise for further applications to biological systems. Specifically, it is of great importance to characterize the fast NLO effects resulting from different pulse durations and intensities and at different wavelengths of operation. This information will help to estimate the water-soluble polymeric dye's capability for applications in two-photon luminescence imaging, trace detection in biological tissue, and enhanced and precise ablation of biological tissue due to nonlinear absorption.

In this paper we present the detailed results of the nonlinear optical properties of the two water-soluble polymeric dyes, R-478 and S-119. The measurements used to investigate the third-order NLO effects of these materials are the open and closed aperture *z*-scan experiments and the nonlinear transmission measurement. The NLO properties of the polymeric systems were investigated with two different pulse durations in the nanosecond and femtosecond regimes. The measurements for nonlinear absorption were also carried out with the polymeric systems in a film geometry. The results of the NLO measurements are compared to other reported systems with large NLO effects, and a figure of merit is provided. For the case of fast electronic NLO effects it is important to probe the origin of the effect in the polymeric dye. NLO measurements were also performed on the chromophore group ("Sunset Yellow" for the case of poly(S-119)), and the results are compared to those obtained from the parent polymer. The utility of the water-soluble polymeric dyes for nonlinear laser ablation is also demonstrated.

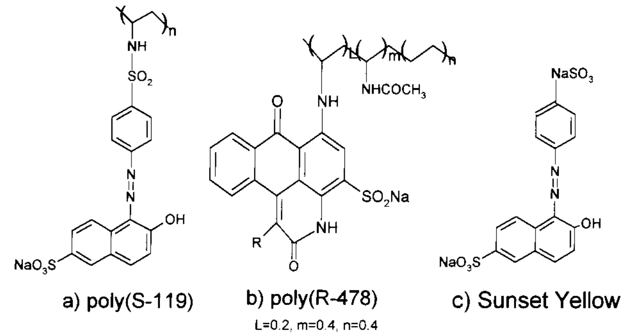

Figure 1. Structure of poly(S-119) (a), poly(R-478) (b), and functional group Sunset Yellow (c) used in this study.

Experimental Section

Characterization of Polymeric Dyes. Our investigations focused on two polymeric systems known by their trade names S-119 and R-478 (molecular structures are shown in Figure 1). The dyes were first synthesized[13a,b] by Dynapol Corp. as food dye candidates. The S-119 dye is an anionic homopolyermeric dye consisting of monomer units of Sunset Yellow. The dye S-119 contains a poly(vinlyamine) backbone and an azo group chromophore. An absorption maximum is observed at 475 nm, and the molar absorptivity is 34.0 $(g/L)^{-1}$ cm^{-1} in aqueous water. The number-average molecular weight of the poly(S-119) is 8.2×10^4 g/mol. The theoretical composition for $(C_{18}H_{14}N_3O_6S_2Na)_n$ was calculated at (C, 47.47; H, 3.10; N, 9.23; S, 14.08). This is comparable to the experimentally found values (C, 46.80; H, 4.05; N, 9.27; S, 13.09).

The second system we investigated was the polymeric dye known by the trade name Poly R-478. Poly R-478 is an anionic anthraquinone dye with a copolymer backbone composed of polyaminoethylene−sodium ethylenesulfonate. The chromophore is an acetylated anthrapyridone. Chromophore attachment to the polymer backbone is 20% mer, 40% mer for the residual amines, and 40% mer for sodium ethylenesulfonate. An absorption maximum is observed at 519 nm, and the molar absorptivity is 13.0 $(g/L)^{-1}$ cm^{-1} in aqueous water. The average molecular weight of the dye is 6.0×10^5 g/mol.

Sample Preparation and Nonlinear Optical Measurements. Solutions were made for most of the NLO measurements with 30 mg of the polymeric dye in 5 mL of H_2O. The solutions were filtered with 0.1 μm filters to remove impurities. Thin films were prepared by spin-coating the polymeric dye solutions in an inert atmosphere. A vacuum oven was used to further aid in water removal from the films. Careful annealing and aging of the films was carried out in order to produce thin films of good optical quality. The absence of water remaining in the films was checked by UV−vis and IR spectroscopy. The thickness of the films was evaluated to be of ~100 μm. The steady-state absorption spectra were obtained with a fiber-optic spectrometer, and the results for the two polymeric dyes can be seen in Figure 2.

The femtosecond NLO experiments were performed using fundamental laser emission from a Ti:sapphire (Tsunami, Spectra Physics) femtosecond laser system pumped by a 5 W CW $Nd:YVO_4$ laser (Millenia, Spectra Physics). This system can deliver stable ultrashort light pulse sequences with individual pulse durations of ~100 fs and at a repetition rate of 82 MHz. The output spectrum of the laser radiation was monitored with a spectrum analyzer (REESE Instruments) which was used as a probe to ensure pure mode-locking regime of the femtosecond laser. The maximum average output laser power obtainable at 790 nm was about 700 mW.

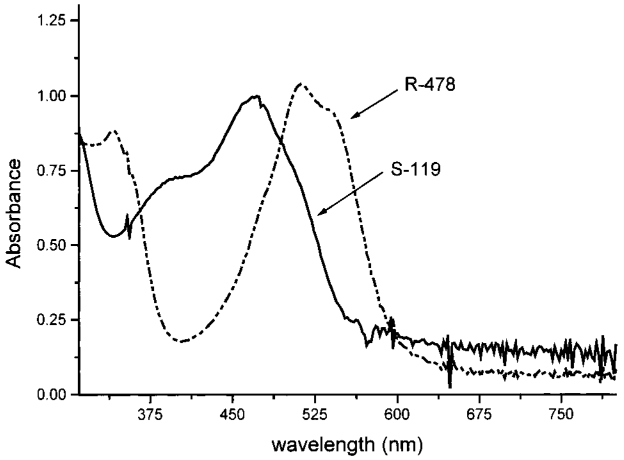

Figure 2. Absorption spectra of S119 and R478 in aqueous solution.

The *z*-scan technique is performed when a Gaussian beam is focused onto the material to induce a nonlinear lens. The presence of this lens influences the beam propagation and distorts its wave front. While the input power is kept constant, the sample experiences a different light field (amplitude and phase) at different *z*-positions. The wave front distortion emerges in beam expansion or contraction in the far field, thus changing the fraction of light passing through the aperture as the sample position is changed. The aperture transmission shows a characteristic peak/valley dependence on *z*-position of the sample.[19] From this dependence one can easily estimate the nonlinear refraction which is related to the nonlinear susceptibility of the material. In the case of relatively small nonlinear phase shifts (and relatively weak nonlinear absorption) it is sufficient to know the difference between normalized peak and valley transmissions $\{T_p - T_v = \Delta T_{pv}\}$.[19–21] By removal of the aperture (in other words, collecting all of the light on the detector), one is able to measure the nonlinear transmission (transmission intensity dependence). This case is referred to as an open-aperture *z*-scan, as opposed to a closed-aperture *z*-scan with the aperture inserted in the far field. In the case of strong nonlinear absorption, when nonlinear variation of normalized transmission in the open-aperture *z*-scan is comparable to the closed-aperture scheme, the signal of nonlinear absorption suppresses the peak and enhances the valley in the closed-aperture *z*-scan.[19,20] If the normalized transmission change caused by nonlinear absorption is small enough, the nonlinear refraction can be estimated from the closed-aperture *z*-scan without additional corrections.[19] An important parameter in the closed-aperture *z*-scan is the aperture nonlinear transmission, $S = 1 - \exp(-2r_a^2/w_a^2)$, where r_a is the aperture radius and w_a is the beam radius at the aperture in the linear regime. This parameter was in our case equal to 0.05. With a circular variable neutral density filter we were able to vary the input beam intensity by more than 2 orders of magnitude, allowing the measurement of the intensity dependence of the *z*-scan effect as well as direct measurement of nonlinear transmission in a wide intensity range.

Time-Resolved Measurements. For fast fluorescence kinetic measurements we apply the femtosecond fluorescence up-conversion technique for time-resolved detection of the luminescence.[22,23] The sample was excited with laser pulses delivered by a frequency-doubled output of a Ti:sapphire laser with a pulse width of about 100 fs tuned at 790−860 nm and a repetition rate of 82 MHz. The temporal profile of the fluorescence was monitored by sum-frequency generation with a delayed reference pulse within a nonlinear crystal of β-barium borate (BBO). The sum-frequency signal was dispersed in a monochromator and detected with a single photon counting unit. The fwhm of the cross-correlation function at 790/395 nm was estimated to be 190 fs. The rotating sample cell and holder (1 mm thickness in the case of solutions) were used to avoid thermal and photochemical accumulative effects. The average concentration used in time-resolved measurements was 0.6 mg/mL. Excitation average power was kept at the level of a few (in most cases ~1 mW) milliwatts. This corresponds to an input pulse energy well below 0.1 nJ at 395 nm. It is important to note that in this excitation intensity (energy) regime the fluorescence kinetics was found to be independent of the excitation intensity (energy) for all investigated polymer solutions.

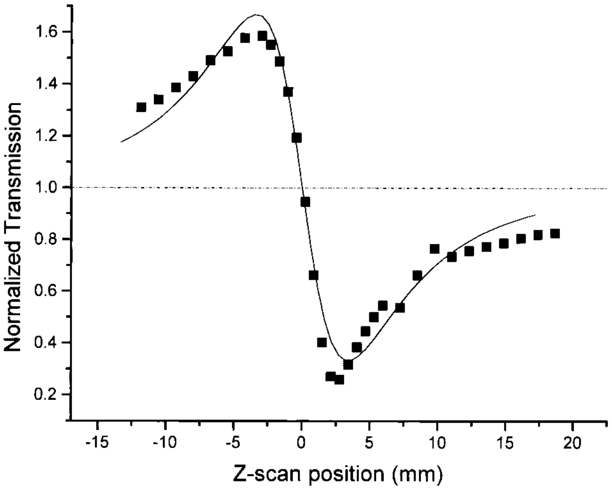

Figure 3. Close-aperture *z*-scan for R478 at incident irradiance 3 GW/cm^2 at 800 nm. Solvent is water and concentration is 1.45×10^{-2} mol/L. The solid line is a theoretical fit.

Results and Discussion

To estimate the fast nonresonant third-order NLO properties of the polymeric dyes, measurements at 800 nm where performed with 100 fs pulses. The closed aperture *z*-scan result of the polymeric dye R-478 at input intensities of 3 GW/cm^2 and with 100 fs pulses is shown in Figure 3. It can be seen that there is a large change in transmission for this system at these peak intensities.

The closed *z*-scan was carried out at different intensities, and the results showed a linear intensity dependence (even at relatively low peak intensities) up to the point of 3.5 GW/cm^2 where the onset of saturation of the NLO effect was observed. The transmission curve was fit to the well-known expression outlined in the literature,[19,20] and the result gives an estimate of the nonlinear refractive index exhibited by the polymer. For the case of the R-478 polymer at 800 nm in solution with 100 fs pulses, we obtain a value of $n_I = 1.26 \times 10^{-4}$ cm^2/GW and a value of the third-order NLO susceptibility of $\chi^{(3)} = 5.7 \times 10^{-12}$ esu. It is important to note that the contribution due to nonlinear refraction of the water solvent has been taken into account for these evaluations. The solvent (water) contribution to the electronic nonlinear refractive index was found to be $n_I = 3.6 \times 10^{-6}$ cm^2/GW. Thus, it can be seen that polymeric dye R-478 exhibits a nonlinear refractive index 2 orders of magnitude larger than that obtained from pure water.

We have also carried out closed *z*-scan measurements in solution of the polymeric dye S-119 (see Figure 1b) utilizing femtosecond pulses. The result of the closed *z*-scan measurement at a peak intensity of 8.6 GW/cm^2 is shown in Figure 4.

Interestingly, although the S-119 polymer has the dipolar azobenzene group and larger conjugation length, it appears to have a smaller nonlinear refraction as compared to the R-478 at this wavelength. Also, the

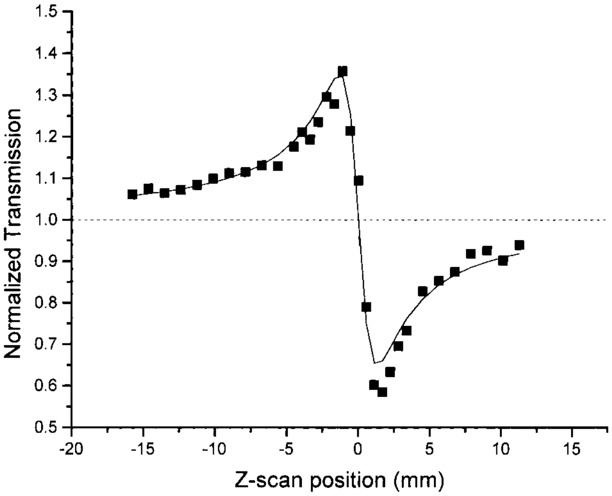

Figure 4. Close-aperture *z*-scans for S119 at incident radiance 8.6 GW/cm^2 at 800 nm. Solvent is water and concentration is 1.38×10^{-2} mol/L. The solid line is a theoretical fit.

peak intensity used in the S-119 measurements (shown in Figure 4) is more than 2 times larger than that used in the R-478 experiments, and the change in transmission amplitude of the S-119 polymeric dye ($\Delta T = 0.773$) is still less than half the value obtained for the R-478 polymeric dye ($\Delta T = 1.242$). The value of the nonlinear refractive index obtained from the S-119 polymeric dye at 800 nm in solution with 100 fs pulses was found to be $n_I = 2.3 \times 10^{-5}$ cm^2/GW, and the third-order NLO susceptibility was calculated to be $\chi^{(3)} = 1.0 \times 10^{-12}$ esu when the contribution from the water was taken into account.

To probe the NLO properties at different wavelength and pulse duration, the two polymeric dyes were investigated at 1064 nm using nanosecond pulses. In this regime the nonlinear refraction results from solutions were only comparable to those obtained with pure solvent (water) and therefore could not provide a clear picture of the nonlinear refraction in the polymeric dyes. The nonlinear absorption effects in solution were also found to be below the detectable limit. However, significant nonlinear absorption effects were observed with nanosecond pulses in thin films of the polymers S-119 and R-478. Our interest for the thin film configuration was motivated by the advantages for device fabrication of nonlinear absorber materials for potential applications in optical limitation.[24] The origin of the nonlinear absorption properties in these polymeric structures may cover a broad range of processes such as two- and three-photon absorption and excited-state absorption.[25,26] In this context, our research has been focused on both the fundamental aspect of understanding the multiphoton mechanisms underlying the nonlinear absorption effects and on the technological attractiveness of these materials as efficient optical limiters at 1064 nm. Multiphoton absorption is an instantaneous process that leads to much faster nonlinear response of the material as compared with light-induced scattering or reverse saturable absorption which have been widely used as optical limiting mechanisms in organic materials.[24,26]

Shown in Figure 5 are the results of the nonlinear transmission measurements of the S-119 and R-478 thin films at 1064 nm, for the incident peak intensities ranging up to ~1.5 GW/cm^2.

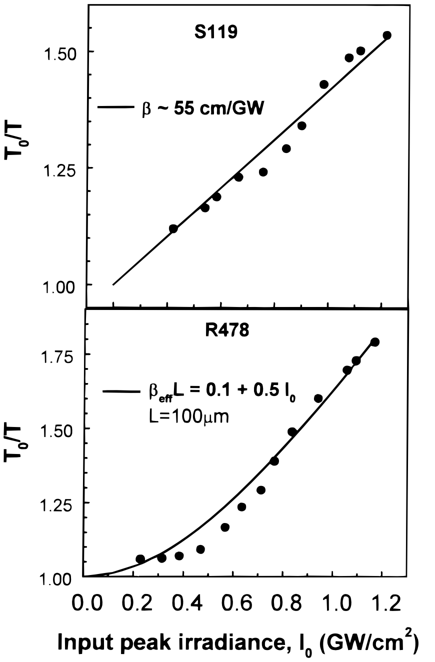

Figure 5. Nonlinear transmission results for the S-119 and R-478 thin films for nanosecond pulse measurements at 1064 nm. The solid lines are theoretical fits according to the case of 2PA for S-119 and according to eq 1 (intensity dependent 2PA) for R-478.

The contribution of multiphoton absorption to the nonlinear transmission data in Figure 5 was analyzed in accordance with the propagation equation of the laser peak intensity.[27] Both the combination of two-photon absorption (2PA) and three-photon absorption (3PA) and the excited-state absorption (ESA) initiated by 2PA can actually determine an overall effect of intensity-dependent 2PA. The particular effect of combined 2PA and 3PA on the nonlinear transmission can be described by the following equation:[26,27]

$$\frac{T_0}{T} = 1 + (\beta + \gamma I_0)LI_0 = 1 + \beta LI_0 + \gamma L(I_0)^2 \quad (1)$$

This is not an exact solution of the plane-wave propagation equation; however, it serves as a phenomenological parametrization of the 2PA coefficient as being intensity dependent when considering combined 2PA and 3PA effects, so that the nonlinear transmission can be characterized by an overall effective 2PA coefficient $\beta_{\text{eff}} = \beta + \gamma I_0$.

In the case of S-119 at 1064 nm in film we obtained a good fit of the nonlinear transmission by assuming the pure contribution of 2PA data (solid line in Figure 5a), as characterized by $\gamma = 0$ in eq 1 and calculated a value as high as 55 cm/GW for the 2PA absorption coefficient β. However, the pure contribution of 2PA appeared not to provide an adequate fit to the nonlinear transmission data for the R-478 polymer film, as seen in Figure 5b. Therefore, we took into account the possibility of higher-order multiphoton processes contributing to the NLO response in R-478. In this respect, we found a good agreement of the experimental nonlinear transmission of the R-478 thin film with eq 1 including all terms. Within this interpretation, the resulting effective 2PA coefficient for R-478 at 1064 nm in film, at a peak intensity of 0.8 GW/cm^2, up to 50 cm/GW.

The values of the nonlinear absorption coefficients calculated from the nonlinear transmission measure-

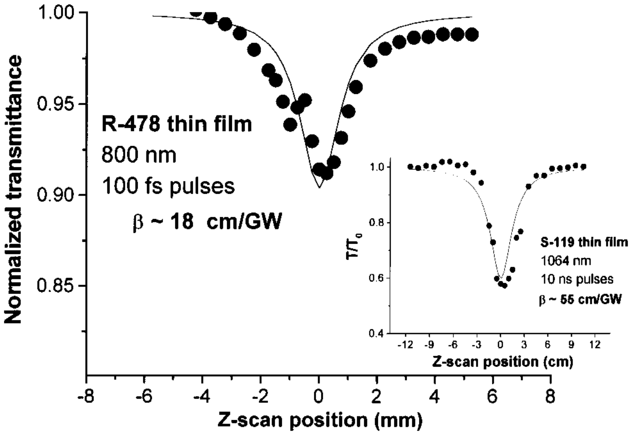

Figure 6. Open *z*-scan data for the R-478 thin film with femtosecond pulses at 800 nm for an incident irradiance of 0.6 GW/cm^2. The solid line is a theoretical fit. The inset shows the open *z*-scan trace for the S-119 thin film at 1064 nm for an input irradiance of 0.8 GW/cm^2.

ments agree well with the results of the open *z*-scan experiments for both samples. To illustrate this, we show in Figure 6 inset the open *z*-scan data for the S-119 thin film at a peak intensity of 0.8 GW/cm^2 at 1064 nm.

The theoretical fit is based on the pure 2PA model. These remarkably high values of the two-photon nonlinear coefficients in both water-soluble polymer films at 1064 nm are backed up by the nonlinear absorption data recorded for femtosecond excitation at 800 nm. The open *z*-scan results for R-478 at 800 nm are shown in Figure 6.

The 2PA coefficients we evaluated in this regime are of ~18 and ~8 cm/GW for R-478 and S-119, respectively, at 800 nm and in film. These coefficients are still relatively large in this femtosecond regime, but the fact that they are lower than for nanosecond excitation at 1064 nm can be assigned to the shift of the excitation wavelength to a spectral domain where the 2PA resonance is reduced. The closed-aperture *z*-scan traces for the thin films were found to be rather noisy and did not give a reliable estimate of the nonlinear refractive indices. These fluctuations of the closed-aperture *z*-scan signal were connected with small optical imperfections in the thin films; it is worth mentioning that the angle-dependent closed-aperture *z*-scan is more sensitive to sample irregularities than the open *z*-scan.[20] However, the large nonlinear absorption coefficients reported above make the thin film configuration of these polymers very promising for optical limiting and intensity discrimination in the optical processing of information. In fact, the 2PA coefficients exhibited by these water-soluble polymer thin films are among the highest so far reported, being comparable to the similar coefficients for the well-known NLO conjugated polymer PPV.[28]

To probe the origin of the fast electronic NLO effects exhibited in the polymeric structures, we investigated model systems containing related chromophore groups. For the case of poly S-119 the smaller azo-chromophore group (Sunset Yellow, SY, shown in Figure 1c) was investigated. NLO measurements were carried out under the same experimental conditions used in the studies of the parent polymer poly(S-119) as described above. The result of the SY closed *z*-scan measurement at 800 nm (100 fs pulses) with the same chromophore concentration as was used for poly(S-119) is shown in Figure 7.

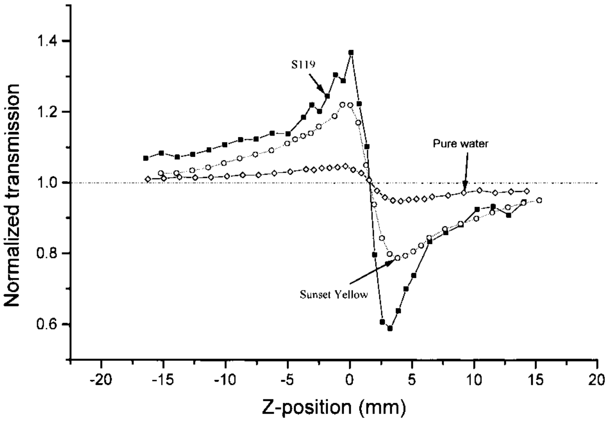

Figure 7. Comparison of close-aperture *z*-scans for S119, Sunset Yellow, and water at 800 nm.

From the closed *z*-scan result shown in Figure 7 the nonlinear refractive index was estimated to be $n_I = 1.2 \times 10^{-5}$ cm^2/GW. The magnitude of the NLO coefficient from the chromophore Sunset Yellow is significantly smaller than that obtained from the full-functionalized polymer sample. The difference in NLO response of the two systems can be clearly seen when they are illustrated together at the same peak intensity and concentration of NLO chromophore as seen in Figure 7. It is interesting to note that both of these materials are stable in the presence of the short pulses and large peak intensities.

The large closed *z*-scan results as well as the large nonlinear absorption detected for the two polymeric dyes are mainly due to fast electronic nonlinear responses of the poly(S-119) and poly(R-478) systems. The contribution of interactions of the NLO chromophores attached to the side chain of the polymer may be used to explain the enhancement of NLO effects in functionalized systems. The polymer experiences an enhanced degree of interactions due to the relatively short interaction distance of the NLO chromophores on the side chain. To probe the fast electronic dynamics, we investigated the ultrafast luminescence decay utilizing upconversion spectroscopy. Our experimental setup and methodology for performing the upconversion experiment has been reported previously (see Experimental Section) and in the literature.[22,23] Shown in Figure 8 is the result for the polymer S-119 (in the solid line) and the chromophore SY (in the dashed line) measured at an emission detected wavelength of 580 nm. For both measurements the excitation wavelength was 395 nm. As it can be seen from Figure 8, the relaxation decay time of the poly(S-119) is rather complex with several different components. The complex relaxation curve of the S-119 probed at 580 nm can be fitted to the equation

$$g(t) = A\mathrm{e}^{-(t/\tau_1)} + B\mathrm{e}^{-(t/\tau_2)} + C\mathrm{e}^{-(t/\tau_3)} \qquad (2)$$

where *A*, *B*, and *C* are constants proportional to the relative magnitude of the contributions of the different mechanisms which are assigned to photoisomerization of the azo-chormophore (short components) and, possibly, to the existence of long-lived species in the polymer (excimer emission). The parameters obtained from the fit to eq 2 (no-linear least-squares procedure with deconvolution) were found to be $A = 0.32$, $\tau_1 = 0.32$ ps, $B = 0.40$, $\tau_2 = 1.38$ ps, $C = 0.28$, and $\tau_3 = 10$ ps. The emission wavelength dependence of the decay curves

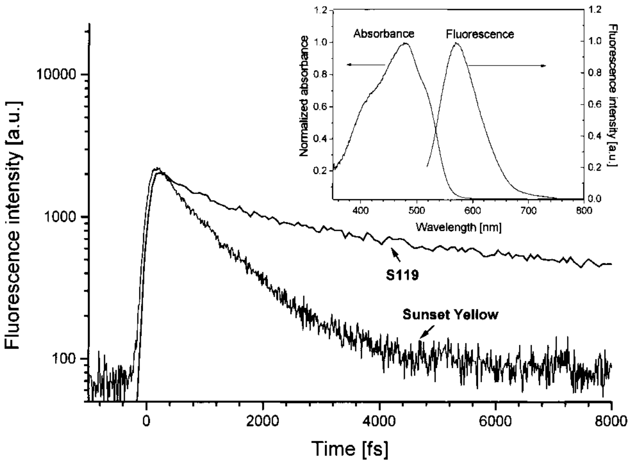

Figure 8. Fluorescence dynamics of poly(S-119) (solid line) and Sunset Yellow (dash) in water. Excitation wavelength is 395 nm. The inset shows the absorption and fluorescence emission spectra of poly(S-119).

was also investigated, and the results showed an increase in the contribution of the long-lived component with increasing emission wavelength for S-119. The importance of the rather complex dynamics gives further proof of additional fast electronic processes and multicomponent dynamics of the polymer ultimately contributing to the observed NLO responses. We have also measured the fast dynamics of the chromophore SY (which is the same chromophore in the S-119 polymer), and the result is also shown in Figure 8. It is clearly seen that the luminescence decay of SY is very different from that of the poly(S-119) and resembles a single-exponential decay. Actually the decay curve can be well fitted to the two-exponential decay function with short time constants of 0.48, 1 ps and relative amplitudes 0.67, 0.33, respectively. The fast decay channel is most probably connected to a photoisomerization process proposed for azobenzene dyes.[29] This relatively large difference in fast dynamics in the two systems (Sunset Yellow and poly(S-119)) suggests that an enhancement of the nonlinear optical properties obtained for the poly(S-119) originates from the interactions of the chromophores on the side chain of the polymer. Although the mean concentration of chromophores is indeed the same for both samples used to obtain the results in Figures 7 and 8, the distance between chromophores is much greater in the case of the Sunset Yellow result. This suggests that the enhancement of the NLO response seen in Figure 7 may arise from the increased intermolecular interaction.

It has been shown that enhanced NLO responses of organic chromophores attached to side-chain polymers[30] as opposed to simple doped guest/host systems can experience a large degree of dipolar interaction due to orientational pair correlation that arises from the angular dependence or anisotropic intermolecular potential between NLO chromophores. Any type of anisotropic intermolecular potential (whether it be short- or long-range interactions) can affect the relaxation of the dipolar chromophore. When the interactions are weak, as in the case of Sunset Yellow, the conformational mobility is relatively fast and unaffected by intermolecular effects. In the case of S-119 there are stronger interactions, and the additional mechanisms seen in the decay curve can be attributed to cooperative processes in the polymeric system during the course of its relaxation. In this case intermolecular interactions can inhibit the fast conformation change as for example in the case of J-aggregate formation.[31] Inhomogeneity due to the curvature of polymer chain, kinks, and other defects can lead in turn to a distribution of lifetimes and complex fluorescence kinetics. The additional longer components for the case of S-119 can be attributed to the formation of aggregates due to the high number density of NLO chromophores attached to the side chain.[23]

As stated above, one of the important reasons why we are so interested in the NLO properties of the two particular polymeric dyes is that they may have strong application in biological systems. Our own interest in these applications involves the ablation of (unwanted) biological tissues by use of nonlinear absorption of embedded photosensitizers. Specifically, there are some advantages of the procedure of nonlinear ablation over the linear case.

Generally, in current surgical procedures laser ablation is carried out with nanosecond high-energy pulses focused onto the tissue directly. While ablation is immediate, the severe effects of large collateral damage caused by the heating due to linear absorption limits the use of the procedure presently. For the case of nonlinear absorption, where the excitation (pump) frequency is outside the linear absorption region, the ablation of tissue is also possible. Here, with the use of focused femtosecond pulses, high peak intensities (with low energy) may give rise to ablation caused by a multiphoton process. Selectivity is added in the fact that the tissue does not absorb the light, but instead the embedded (doped) polymeric dyes absorb the light in a nonlinear manner that is dependent upon the input intensity. This could ultimately lead to a much smaller amount of collateral damage and eventually for practical application in surgery.

We began investigations in the use of the polymeric dye R-478 in A549 cells (lung carcinoma cells) for ablation experiments. The cells were treated with R-478 polymer mixed in RPMI1640 (without phenol red) and 1% fetal calf serum (FCS). The exposure time of the cells to R-478 was then varied as was the R-478 drug concentration. The media was removed, and cells were washed with PBS. The absorbance for each sample was measured at 510 nm.

The results shown in Figure 9 illustrate that with an increase in absorbance at 510 nm there is an increase in polymeric dye R-478 content. This demonstrates that after several washings a significant content of R-478 remained. The nature of the drug−polymer interaction is still a matter of investigation. At a concentration of approximately 5 mg/mL no further increase in absorption at 510 nm was observed. This indicates a saturation of the drug−cell interaction. Because of practical considerations, we chose 0.5 mg/mL as the drug concentration used in our studies. The inset of Figure 9 shows the effect of various incubation times of the cells with the polymeric dye. The absorbance at 510 nm was also monitored as a function of incubation time. We found that 3 h was the optimal incubation time. At this time duration no cell death could be attributed to the drug alone. Using a hemocytometer, a constant number of cells were counted, and a portion of them were exposed to the drug at 0.5 mg/mL for 3 h. After the incubation time, the residual (uninteracted) dye was washed away with PBS.

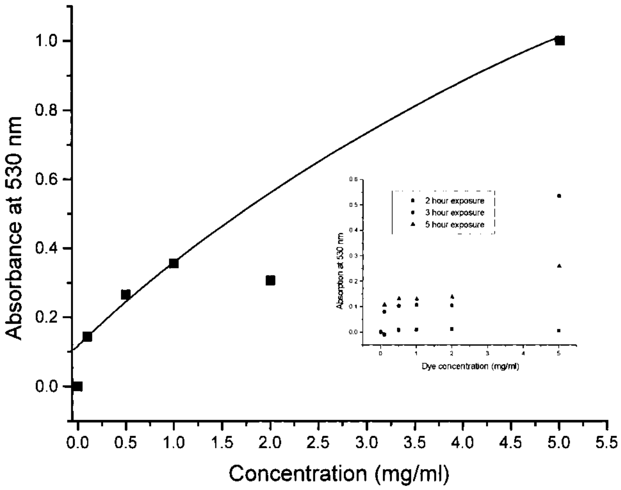

Figure 9. Absorbance of A549 lung carcinoma cells incubated with varying concentrations of poly(R-478). Inset shows the effect of different incubation times.

The cells were exposed to a Ti:sapphire laser (8 nJ/pulse with 100 fs pulses at 800 nm). We adjusted the spot size to be the same as the area of one of the 96 plate wells at 0.79 cm^2. Different experiments were performed at various intensities with femtosecond pulses. In a number of experiments low-intensity (0.08 GW/cm^2) excitation was used while in a number of other experiments higher intensities were used (0.8 GW/cm^2). After laser exposure, the cells were incubated at 37 °C over a time course lasting 3 days. Each day, a number of cells were harvested, and they were tested for cell mortality. The MTT (#9) colorimeteric test[32] was used to compare the living cells with those killed by the nonlinear absorption process at a wavelength of 560 nm. From these results we can determine the relationship between cell vitality and the application of both the laser and the nonlinear absorbing polymeric dye R-478. When no drug was applied but high-intensity femtosecond laser pulses were applied, the cell vitality was not effected. For the cells that were treated with the R-478 drug but not exposed to femtosecond laser pulses, the number of remaining viable cells did not change. However, for the cells treated with both the drug and with laser, the number of viable cells after irradiation of femtosecond pulses were dramatically reduced. The reduction in viable cells due to the application of laser with drug was approximately the same at 15%. This result shows that the cells were reduced by the excitation of the polymeric NLO dyes in the nonlinear absorbing regime. The result demonstrates our general method of nonlinear ablation of biological tissues.

Conclusions

We have measured large nonlinear optical properties of two novel water-soluble organic polymeric dyes. Thin films of poly(S-119) film showed large nonlinear absorption in the infrared with a two-photon absorption coefficient of 55 cm/GW. Also, the two-photon absorption coefficient of the R-478 polymer thin film probed with femtosecond pulses at 800 nm was 18 cm/GW. At relatively moderate peak intensities these values of the nonlinear absorption are certainly significant and appropriate for potential NLO applications. The mechanism of the enhanced NLO effect in the S-119 polymer solution is attributed to intermolecular dipole−dipole interactions. This was experimentally determined by the comparison of the NLO and time-resolved luminescence responses of the smaller chromophore group Sunset Yellow with the pristine polymer S-119. The nonlinear refraction and relaxation dynamics were significantly smaller and less complex for the chromophore compared to the polymer. These polymers have potential applications for the characterization and laser ablation of biological systems such as neoplastic cells. Our results at 800 nm and with 100 fs pulses in lung carcinoma cells treated with the R-478 polymeric dye have demonstrated the mechanism of nonlinear ablation. We have observed that when the cells are treated with R-478 and are exposed to femtosecond laser light, a 15% reduction in cell vitality was obtained. We also found that without the use of the R-478 polymeric dye but with laser exposure there was no significant change in cell vitality.

Acknowledgment. This work was supported in part by the NSF, Grant DMR-9908418.

References and Notes

(1) Sariciftci, N. S. *Prog. Quantum Electron.* **1995**, *19*, 131−159.
(2) Bao, Z.; Rogers, J. A.; Dodabalapur, A.; Lovinger, A. J.; Katz, H. E.; Raju, V. R.; Peng, Z.; Galvin, M. E. *Opt. Mater.* **1999**, *12*, 177−182.
(3) Dai, L. M. *Polym. Adv. Technol.* **1999**, *10*, 357−420.
(4) Blatchford, J. W.; Epstein, A. J. *Am. J. Phys.* **1996**, *64*, 120−135.
(5) Heflin, J. R.; Figura, C.; Marciu, D.; Liu, Y.; Claus, R. O. *Appl. Phys. Lett.* **1999**, *74*, 495−497.
(6) Yitzchaiks; Roscoe, S. B.; Kakkar, A. K.; Allan, D. S.; Marks, T. J.; Xu, Z. Y.; Zhang, T. G.; Lin, W. P.; Wong, G. K. *J. Phys. Chem.* **1993**, *97*, 6958−6980.
(7) Katz, H. E.; Scheller, G.; Putvinski, T. M.; Schilling, M. L.; Wilson, W. L.; Chidsey, C. E. D. *Science* **1991**, *254*, 1485−1487.
(8) Lvov, Y.; Yamada, S.; Kunitake, T. *Thin Solid Films* **1997**, *300*, 107−112.
(9) Wang, X. G.; Balasubramanian, S.; Li, L.; Jiang, X. L.; Sandman, D. J.; Rubner, M. F.; Kumar, J.; Tripathy, S. K. *Macromol. Rapid Commun.* **1997**, *18*, 451−459.
(10) Tian, H. J.; Mao, H. F.; Zhou, Q. F.; Xu, H. J.; Si, J. H.; Wang, Y.; Yang, Q.; Ye, P. X. *Chem. Phys. Lett.* **1996**, *263*, 471−475.
(11) Fox, J. M.; Katz, T. J.; Van Elshocht, S.; Verbiest, T.; Kauranen, M.; Persoons, A.; Thongpanchang, T.; Krauss, T.; Brus, L. *J. Am. Chem. Soc.* **1999**, *121*, *14*, 3453−3459.
(12) Girling, I. R.; Cade, N. A.; Kolinsky, P. V.; Jones, R. J.; Peterson, L. R.; Ahmad, M. M.; Neal, D. B.; Petty, M. C.; Roberts, G. G.; Feast, W. J. *J. Opt. Soc. Am. B* **1987**, *4*, 950.
(13) (a) Dawson, D. *Alderichim. Acta* **1981**, *14*, 22−29. (b) Dawson, D. J.; Gless, R. D.; Wingard, R. E. *J. Am. Chem. Soc.* **1976**, *98*, 5996−5999.
(14) Stahl, G. E.; Fayer, J. C.; Ning, S. C.; Watkins, J. B. *J. Pediatr. Gastroenterol. Nutr.* **1991**, *12*, 485−493.
(15) Ball, A. S.; Calton, J. *J. Basic Microbiol.* **1996**, *36*, 13−18.
(16) Tucker, B.; Radtke, C.; Kwon, S. I.; Anderson, A. J. *J. Hazard. Mater.* **1995**, *41*, 251−265.
(17) Baldrian, P.; Gabriel, J.; Nerud, F. *Folia Microbiol.* **1996**, *41*, 363−367.
(18) Figaro, J.; Ispasoiu, R.; Varnavski, O.; Pass, H.; Goodson, T., to be published.
(19) Sheik-Bahae, M.; Said, A. A.; Wei, T.; Hagan, D.; Van Stryland, E. W. *IEEE J. Quantum Electron.* **1990**, *26*, 760−769.
(20) Chapple, P. B.; Staromlynska, J.; Hermann, J. A.; McKay, T. J. *J. Nonlinear Opt. Phys. Mater.* **1997**, *6*, 251−293.
(21) Sheik-Bahae, M.; Said, A. A.; Van Stryland, E. W. *Opt. Lett.* **1989**, *14*, 955−997.
(22) Shah, J. *IEEE J. Quantum Electron.* **1988**, *24*, 276−288.
(23) Varnavsky, O.; Leanov, A.; Liu, L.; Takacs, J.; Goodson, T., III Submitted for publication.
(24) Tutt, L. W.; Boggess, T. F. *Prog. Quantum Electron.* **1993**, *17*, 299−338.
(25) Shim, H.; Liu, M.; Hwangbo, C.; Stegeman, G. I. *Opt. Lett.* **1998**, *23*, 430−432.
(26) Sun, Y. P.; Riggs, J. E. *Int. Rev. Phys. Chem.* **1999**, *18*, 43.

(27) Boggess, T. F.; Bohnert, K. M.; Mansour, K.; Moss, S. C.; Boyd, I. W.; Smirl, A. L. *IEEE J. Quantum Electron.* **1986**, *22*, 360−368.

(28) Samoc, M.; Samoc, A.; Luther-Davies, B.; Bao, Z.; Yu, L.; Hsieh, B.; Scherf, U. *J. Opt. Soc. Am. B* **1998**, *15*, 817−825.

(29) (a) Lednev, I. K.; Ye, T. Q.; Abbott, L. C.; Hester, R. E.; Moore, J. N. *J. Phys. Chem. A.* **1998**, *102*, 9161−9166. (b) Lednev, I. K.; Ye, T.-Q.; Hester, R. E.; Moore, J. N. *J. Phys. Chem.* **1996**, *100*, 13338−13341.

(30) Goodson, T., III.; Wang, C. W. *Macromolecules* **1993**, *26*, 1837−1840.

(31) (a) Horng, M. L.; Quitevis, E. L. *J. Phys. Chem.* **1993**, *97*, 12408−12415. (b) Reid, P. J.; Higgins, D. A.; Barbara, P. F. *J. Phys. Chem.* **1996**, *100*, 3892−3899.

(32) Chen, H.; Zhang, Z. S.; Zhang, Y. L.; Zhou, D. Y. *Anticancer Res.* **1999**, *19*, 3675−3680.

MA991868G